

## **Chapter V**

### **A Study as a Multifunctional Additives of Acrylate Based ZnO Nano Composite for Lubricating Oil**

### 1.5.1 Introduction

Service life, economic efficiency, and engine operation are directly or indirectly depend on the quality, performance, and sensible use of the oils [1], [2]. The two major constituents of tribology are friction and wear. The service of the machine automatically increases when this friction and wear under controlled and reduced. This ultimately saves money. The awareness of the subject, i.e. identification of tribological problems and their proper solution can give rise to a considerable saving. According to some estimation, losses due to unawareness of tribology are about 6 % of its gross national product in the United States. Thus the significance of friction reduction and wear management cannot be overemphasized for economic reasons and long-term dependability. In this regard, researchers are focused on the application of nanoparticles (NPs) in lube oil. Nanoparticles blended lubricating oils can boost the properties of extreme pressure anti-wear, and friction reduction capability and hence improved the service life of the machine [3]. The anti-wear and friction reduction action is depended on the characteristics of nanoparticles, for example, shape, size, and concentration. Due to its large surface area nanoparticles are dissimilar from other materials. As a result, nanoparticles are very reactive compared to their bulk form. Now a day, generally used nanoparticles are oxides based-  $\text{Al}_2\text{O}_3$ ,  $\text{CuO}$ ,  $\text{ZnO}$ , metals-  $\text{Al}$ ,  $\text{Cu}$ , nonmetals- graphite, carbon nanotubes, layered composites-  $\text{Al}-\text{Al}_2\text{O}_3$ ,  $\text{Cu}+\text{C}$ , functional nanoparticles, etc. Due to their unique structure and performance,  $\text{ZnO}$  nanoparticles have been attracted considerable interest among different kinds of nanoparticles [4]-[7].  $\text{ZnO}$  nanoparticle has a huge surface area, high surface energy, high diffusion, strong adsorption characteristics. Apart from that,  $\text{ZnO}$  NPs have attracted increasing attention because these NPs can be easily synthesized and it is a greener material i.e, biocompatible and nontoxic [8]. Nano-sized base oil additives are

appropriate for heavy load, low speed, high-temperature work, and have excellent extreme pressure resistance, and anti-wear resistance performance, and better lubrication properties. When ZnO nanoparticles are used as lube oil additive, not only enhance the tribological properties of base oils but also potentially reduce the cost of lube oil. On the other hand, due to its hydrophilic-oleophobic nature, nano-ZnO is poor oil soluble. It needs to depend on the role of dispersant, ultrasonic dispersion, or strong agitation to disperse nano-ZnO particles in the base oils [9]-[13]. So, nano-ZnO particles alone do not show other kinds of additive performance. Therefore, to disperse ZnO nanoparticles to lube oil to develop a multifunctional performance additive, ZnO nanoparticles were first dispersed acrylate-based polymer matrix by sonication. Since acrylate-based polymer was known to perform as a good viscosity index improver [14]-[16] and pour point depressant [17]. The main objective of this research work is to study the multifunctional additive property of polymer-ZnO nanocomposites for lube oil. In our previous work, we made a polyacrylate-nano magnetite composite [18] and polyacrylate-Liquid crystal composite [19] to study the multifunctional additive performance. In continuation of our work, here we have introduced nano ZnO into the polyacrylate system to study the multifunctional additive properties (tribological performance, viscosity index improver, pour point depressant) of this polymer-ZnO nanocomposite.

## **1.5.2 Experimental Section**

### **1.5.2.1 Materials and methods**

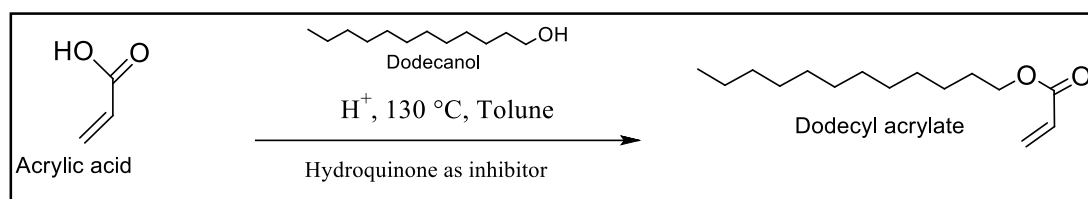
Dodecyl alcohol, acrylic acid, hydroquinone, and BZP were purchased from Merck specialties Pvt. Ltd. India. Toluene, Methanol, hexane, and conc. H<sub>2</sub>SO<sub>4</sub> was purchased from Thomas baker Pvt. Ltd. India. BZP was recrystallized from CHCl<sub>3</sub>-MeOH.

NaOH and ZnCl<sub>2</sub> were purchased from Merck specialties Pvt. Ltd. India. The base oil was collected from the IOCL, Dhakuria, Kolkata, India.

### 1.5.2.2 Preparation of dodecyl acrylate by esterification

Dodecyl acrylate (DDA) was prepared by the esterification process of dodecyl alcohol with acrylic acid in the mole ratio of 1:1.1. The reaction was performed in a resin kettle in the presence of concentrated sulfuric acid as a catalyst, 0.25% hydroquinone is added with respect to the reactants as a polymerization inhibitor, and toluene used as a solvent. The reaction was performed under a nitrogen atmosphere. The reaction mixture was heated gradually from room temperature to 130<sup>0</sup>C using a well-controlled thermostat. The extent of the reaction was monitored by observing the amount of liberated water during the reaction to give the ester, dodecyl acrylate (DDA).

#### Scheme 1.5.1 reaction for the preparation of dodecyl acrylate



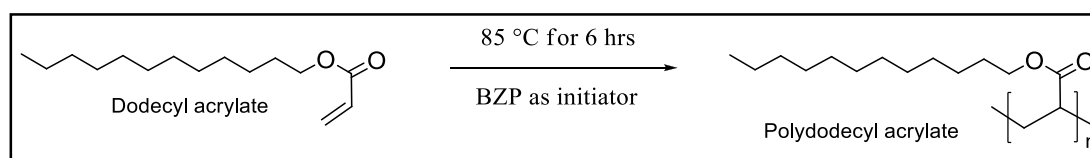
### 1.5.2.3 Purification of the prepared monomer

A desired amount of charcoal was added to the ester to purify the product. After that, it was reflux for 3 h and then filtered. The filtrate was washed frequently with 0.5N sodium hydroxide solution to ensure the complete removal of unreacted acid. Then to remove traces of sodium hydroxide, purified ester was washed several times with distilled water. The prepared ester was then left on calcium chloride overnight and recollected by distillation under reduced pressure. This purified ester was used in the polymerization reaction.

### 1.5.2.4 Preparation of homopolymer of dodecyl acrylate

The polymerization was carried out in a four-necked round bottom flask furnished with a condenser, stirrer, thermometer, and an inlet for the nitrogen insertion. The required amounts of dodecyl acrylate and benzoyl peroxide (BZP) as initiator were taken in the flask and toluene was also added as a solvent. The reaction temperature was controlled at 85<sup>0</sup>C for 6 hours. After that, the reaction mixture was added into methanol solvent with constant stirring to cease the polymerization, and then a precipitate appeared. The precipitate (the polymer) was further purified by frequent precipitation with methanol followed by drying under vacuum at 40<sup>0</sup>C.

#### Scheme 1.5.2 Reaction for the preparation of homopolymer of dodecyl acrylate



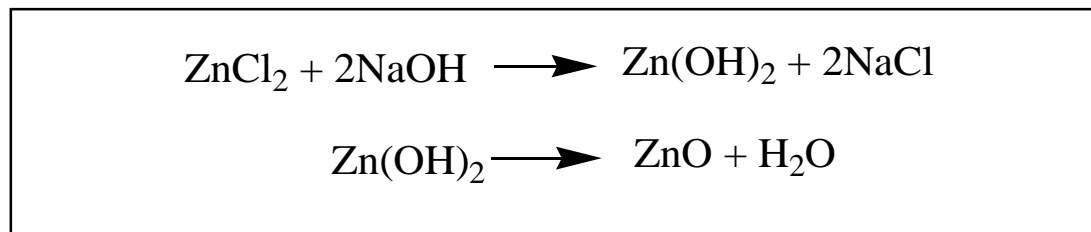
### 1.5.2.5 Preparation of ZnO nanoparticle

5.5 g of ZnCl<sub>2</sub> was dissolved in 100ml of distilled water in a beaker. The solution was kept under constant stirring with a magnet till ZnCl<sub>2</sub> dissolved in the distilled water. The temperature of the solution was increased to 90<sup>0</sup>C by electric hot plate heating. Meanwhile, 20 g of NaOH was dissolved in 100ml of distilled water in a separate vessel. From the prepared NaOH solution, 16 ml of NaOH is added to the beaker with constant stirring, drop by drop through the inner wall of the beaker. Without any precipitation, the aqueous solution turned into a milky white colloid. After completing the addition of NaOH, the reaction was allowed to proceed for another 2 hrs. After completion of the reaction, the solution was allowed to settle and the supernatant solution was removed by washing with distilled water 5 times. After washing, the ZnO

nanoparticles were dried at 100<sup>0</sup>C for 30 min. and then changed into powder form [20].

The reaction involved is given below:

**Scheme 1.5.3 Reaction involved during synthesis of nano-ZnO**



**1.5.2.6 Preparation of poly dodecyl acrylate- ZnO nanocomposites**

PDDA- ZnO nanocomposites were prepared by mixing the PDDA/toluene solution and nano- ZnO particles. The PDDA- ZnO suspension was prepared as follows: 5g of PDDA were dissolved in toluene and the required amount (0.5, 1, and 1.5mg) of nano- ZnO particles were added into the PDDA/toluene solution under the ultrasonic wave and vigorous stirring to prepare 100, 200 and 300 ppm blend and it is depicted in **Table 1.5.2**. The suspension was then poured into a glass plate and allows the toluene to evaporate naturally and a semi-solid mass of polymer-nanocomposites was obtained.

**1.5.3 Measurements**

IR spectra were recorded on a Shimadzu FT-IR 8300 spectrometer using 0.1 mm KBr cells at room temperature within the wavenumber range of 400–4000 cm<sup>-1</sup>. NMR spectra were recorded in Bruker Advance NEO 400 MHz FT-NMR spectrometer using a 5 mm BBO probe using CDCl<sub>3</sub> as solvent and TMS as reference material.

**1.5.3.1 Characterization of nano- ZnO by SEM, X-RD, and DLS**

The synthesized ZnO-nanoparticles were characterized by Field Emission Scanning Microscope (FE-SEM, INSPECT F50, FEI) and XRD analysis is recorded using an

Advance D8, Bruker instrument with  $2\theta$  angle from the range of  $20-90^\circ$ . The DLS of the suspension was performed on a Malvern Zetasizer ver 6.01. For the DLS study suspension of NPs in water was prepared by taking a concentration of 5 mg/mL.

### **1.5.3.2 Determination of molecular weight by GPC**

By GPC, the number average molecular weight ( $M_n$ ) and weight average molecular weight ( $M_w$ ) was determined. The polydispersity index was also calculated. In this method HPLC grade THF (0.4%, w/v) was used as mobile phase in the water 2414 GPC system (polystyrene calibration) at  $35^\circ\text{C}$  with a flow rate of 1 ml/min and the injection volumes are set to 20  $\mu\text{L}$ . The data of this study is given in supporting information.

### **1.5.3.3 Thermogravimetric analysis (TGA)**

The thermal stabilities of the prepared homopolymer and polymer nanocomposites were determined by a thermogravimetric analyzer (Shimadzu TGA-50) using an alumina crucible in air. The system was run at a heating rate of  $10^\circ\text{C}/\text{min}$ . The percentage of weight loss (PWL) with the rise in temperature was calculated.

### **1.5.3.4 Evaluation as viscosity modifier**

The viscosity index (VI) of the polymeric additives was determined in a paraffinic base oil to evaluate the efficiency of the prepared polymeric additives as viscosity modifiers (VM). The viscosity index (VI) of different concentrations of the additives in the base oils was evaluated in two base oils according to the ASTM D2270 method and following the equations as reported by Tanveer and Prasad [21]. Five different concentrations ranging from 1 wt % to 5 wt % of the polymeric sample solutions were used to study the effect of additive concentration on VI.

### 1.5.3.5 Evaluation as pour point depressant

The pour point depressant property of the prepared polymeric additives was determined in base oil by the pour point test on a Cloud and Pour Point Tester model WIL-471(India) according to the ASTM D97 method. In this case, also five different concentrations of the additives were used for each sample.

### 1.5.3.6 Evaluation of the tribological performance of prepared additives

The anti-wear performance of the lubricant compositions was evaluated in terms of wear scar diameter (WSD) by Four-ball wear test apparatus (FBWT) following the ASTM D 4172-94 method [22]. In this experiment 392 N (40 kg) load was applied at 75°C for 30 min. to measure the wear scar diameter (WSD). The diameter of the balls was 12.7 mm and the rotating speed was 1200 rpm. The detailed procedure is described in our publication elsewhere [23].

## 1.5.4 Results and discussion

### 1.5.4.1 Spectroscopic analysis

The FT-IR spectrum of homopolymer dodecyl acrylate (A) and its nanocomposites (Z-3) is shown in **Figure 1.5.1**. The absorption band (**Figure 1.5.1a**) at  $1734.56\text{ cm}^{-1}$  indicated the ester stretching vibration along with other peaks at 1458.40, 1169.67, 1070.96,  $721.65\text{ cm}^{-1}$ . **Figure 1.5.1b** of polymer/ZnO nanocomposites showed absorption band for ester carbonyl group at  $1728\text{ cm}^{-1}$  along with other peaks at 1465.98, 1167.99, 1070.96,  $721.63\text{ cm}^{-1}$ . This shifting of carbonyl stretching frequency may be due to some association of nano magnetite and poly dodecyl acrylate. The peaks in the range at 1458.40,  $1465.98\text{ cm}^{-1}$  are for asymmetric and symmetric bending vibrations of C-H bonds of  $-\text{CH}_3$  and  $-\text{CH}_2-$  groups of polymers and its nanocomposites. Peaks in the range of 1169.67, 1167.99,  $1070.96\text{ cm}^{-1}$  are due

to C-O stretching vibration of the carboxylate ester group. Peaks at about  $721\text{ cm}^{-1}$  are for C-H bending vibration of the paraffinic chain. Broad peaks in the range  $2924.08$  to  $2937\text{ cm}^{-1}$  are for stretching vibration of paraffinic C-H bonds of  $-\text{CH}_2-$  groups. In the infra-red region, the peaks at  $454.6\text{ cm}^{-1}$  correspond to Zinc oxide nanoparticles which show the stretching vibration of Zn-O bond [24]. There is no significant peak observed in the range of the carbon-carbon double bonds region which supported the formation of the polymer.

The  $^1\text{H}$  NMR spectra of A and Z-3 are shown in **Figure 1.5.2** & **Figure 1.5.2a** represents the spectrum of A which showed broad singlet centered at 4.013 to 4.293 ppm due to the protons of  $-\text{OCH}_2$  group. Methyl protons of the dodecyl chain appeared between 0.866 ppm and 0.878 ppm and the absence of singlet between 5 ppm and 6 ppm implies the absence of any vinylic proton in the polymer. The  $^1\text{H}$  NMR of polymer nanocomposites (**Figure 1.5.2b**) showed a peak at 4.001 and 3.627 ppm due to the protons of  $-\text{OCH}_2$  group of the acrylate polymer and methyl and methylene protons appeared in the range of 0.851 to 0.884 ppm.

In the  $^{13}\text{C}$  NMR spectrum of A, the carbonyl carbon appeared at 174.3 ppm along with other  $\text{sp}^3$  carbons appeared in the range of 64.72 to 13.94 ppm and it is shown in **Figure 1.5.3**. The ester carbonyl of the nanocomposite (Z-3) appeared at 174.5 ppm as shown in **Figure 1.5.3b**. Peaks appeared in the range from 65 to 14.19 ppm are for the  $\text{SP}^3$  carbons of alkyl chains of PNC. The intensity of peaks decreases compared to the pure polymer as depicted in NMR spectra. Hence it can be concluded that ZnO nanoparticles formed a co-ordinate type of bond with ester group of A which lower the stretching frequency of ester carbonyl.

#### 1.5.4.2 Characterization of nano- ZnO (by XRD, SEM, and DLS)

**Figure 1.5.4** shows the X-ray diffraction pattern of ZnO nanoparticles. The nanoscale range of particles in the prepared materials was indicated by a definite line broadening of the X-RD peaks. The eight most intense diffraction peaks located at  $31.84^\circ$ ,  $34.52^\circ$ ,  $36.33^\circ$ ,  $47.63^\circ$ ,  $56.71^\circ$ ,  $62.96^\circ$ ,  $68.13^\circ$ , and  $69.18^\circ$  have been observed which is in good agreement with a research work published elsewhere [25]. Moreover, it also suggests that the synthesized nanoparticles were free of impurities as it does not show any characteristics of XRD peaks other than nano-ZnO peaks. **Figure 1.5.5** represents the scanning electron micrograph (SEM) of the ZnO nanoparticles at different magnifications. These SEM pictures substantiate the formation of ZnO nanoparticles. These pictures confirm the approximately spherical shape of the ZnO nanoparticles. It also can be seen from the pictures that the size of the nano-ZnO is in the range of 15 to 20 nm. The intensity plot showed the relative intensity of light scattered by ZnO NPs. DLS measures the hydrodynamic diameter of the particles. The plot showed only one peak with a mean hydrodynamic size (Z-Average) of 474.6 nm and PDI 0.713. The obtained particle sizes are bigger than those shown in the SEM images due to the agglomeration of the particles [26]. The plot of the size distribution report by the intensity of ZnO NPs as obtained by the experiment was mentioned in the supporting information.

#### 1.5.4.3 Thermogravimetric analysis

The TGA data of the polymer (A) and polymer/ZnO nanocomposites (Z-1, Z-2, and Z-3) are represented in **Figure 1.5.6**. It was seen from the figure that, the thermal stability of all nano blended composites is higher than that of A. At  $380^\circ\text{C}$ , the

percentage of decomposition of the polymer (A) and nanocomposites from Z-1 to Z-3 was 32.42%, 22.88%, 22.09%, and 21.29% respectively, whereas, at 490°C, the percent of weight loss of A, Z-1, Z-2, and Z-3 was 93.71%, 74.86%, 74.08%, and 73.27% respectively. Hence thermal stability of the polymer/ZnO nanocomposites (Z-1, Z-2, and Z-3) was improved by dispersion of the nano-ZnO into the A. This enhancement of thermal stability may be due to the reduction of the mobility of the polymer chain and the tendency of nanoparticles to remove free radicals [27]

#### 1.5.4.4 Efficiency of additive as viscosity modifier

**Figure 1.5.7** represents the viscosity index values of the lubricants blended with the additives. It is observed that the viscosity index (VI) values of the polymer/nano-ZnO composites of different compositions (Z-1, Z-2, and Z-3) at different concentration levels are better than the pure polymer (A). Again with both types of additives, there is always a steady increase of VI values with the increase in additive concentration. An increase in the concentration of the additives leads to an increase in the total volume of polymer micelles in the solutions. The additional increase of volume compared to the pure polymer may be due to the fact that the nanoparticles present in the polymer matrix lead to the polymer chain separated from each other. For all concentrations, the viscosity index values of the prepared polyacrylate-ZnO nanocomposites are higher than polyacrylate- magnetite nanocomposites. The values of the viscosity index of polyacrylate-magnetite nanocomposites are reported in our previous work [18].

#### 1.5.4.5 Efficiency of additive as pour point depressant

Different level of percentage concentration varying from 1 wt% to 5 wt% of the additives in the base oil was tested as PPD and the results are depicted in **Figure 1.5.8**. The results showed that the additives (A, Z-1, Z-2, and Z-3) are efficient as PPD and

the efficiency decreases with increasing additive concentration. The PPD property of all the blended composites is very similar to that of A. That means, incorporation of nanoparticles into the polymer matrix does not affect the PPD property compared to polymer (A). The decrease of pour point is only significant at low concentration (1%). Battez et. al, reported that with higher concentration ( more than 0.4 wt%) of the ZnO NPs, no changes in the pour point have been observed [28], [29]. As reported earlier in our previous work, the pour point depressant property of polyacrylate-magnetite nanocomposites is more or less the same as studied with polyacrylate-ZnO nanocomposites [18].

#### **1.5.4.6 Tribological performance**

The tribological properties of all the lubricant compositions (A, Z-1, Z-2, and Z-3) were determined by measuring WSD by FBWT apparatus employing 40 kg load and the results were depicted in **Figure 1.5.9**. The AW performance of the base oil is significantly enhanced when the additives are blended with it and is indicated by the lower WSD values of the lubricant compositions. The nano-ZnO blended composites exhibited better anti-wear performance compared to only polymer (A) and the performance becomes increasingly better with increasing the number of nanoparticles in the polymer matrix as is shown in **Figure 1.5.9**. The tribological performance of all the lubricant compositions was excellent but less significant than polyacrylate-magnetite nanocomposites as reported in our previous work [18].

#### **1.5.5 Conclusion**

In this study, nano-ZnO was synthesized with better size distribution (15-20 nm) which was established and characterized by SEM, XRD, and DLS study. The interaction of nano-ZnO with PDDA was studied by FT-IR analysis and it suggests that there is

definite interaction between them. All the ZnO nanoparticles blended composites showed excellent performance as anti-wear and viscosity modifier additives for lube oil but they did not improve the pour point significantly compared to pure polyacrylate. Moreover, the thermal stability of polymer was also improved by the incorporation of nano ZnO into the polymer matrix as shown in the thermogravimetric analysis. This change in the properties of the polymer is also evidence of nano-polymer interaction in the blended composites. This study clearly put more insight into the formulation of nano-based multifunctional lubricating oil additives. Therefore, the above study is definitely a potential approach to design multifunctional additives for lubricating oil with better thermal stability.

### **1.5.6 References**

References are given in *BIBLIOGRAPHY* under “Chapter IV of Part I” (Page No. 143-144).

### 1.5.7 Tables and Figures

**Table 1.5.1: Properties of base oil**

<i>Properties</i>	<i>Base oil</i>
Density(kg.m <sup>-3</sup> ) at 313K	918.68
Viscosity (cSt) at 313K	20.31×10 <sup>-6</sup>
Viscosity (cSt) at 373K	3.25×10 <sup>-6</sup>
Viscosity index	89.02
Cloud point (°C)	-8
Pour point (°C)	-6
<i>cSt: centistoke</i>	

**Table 1.5.2: Designation and Composition of polydodecylacrylate nano ZnO composites**

<i>Designation</i>	<i>Composition</i>	
	Polymer in g	Nano (ZnO) in mg
A	5	0
Z-1	5	0.5
Z-2	5	1
Z-3	5	1.5

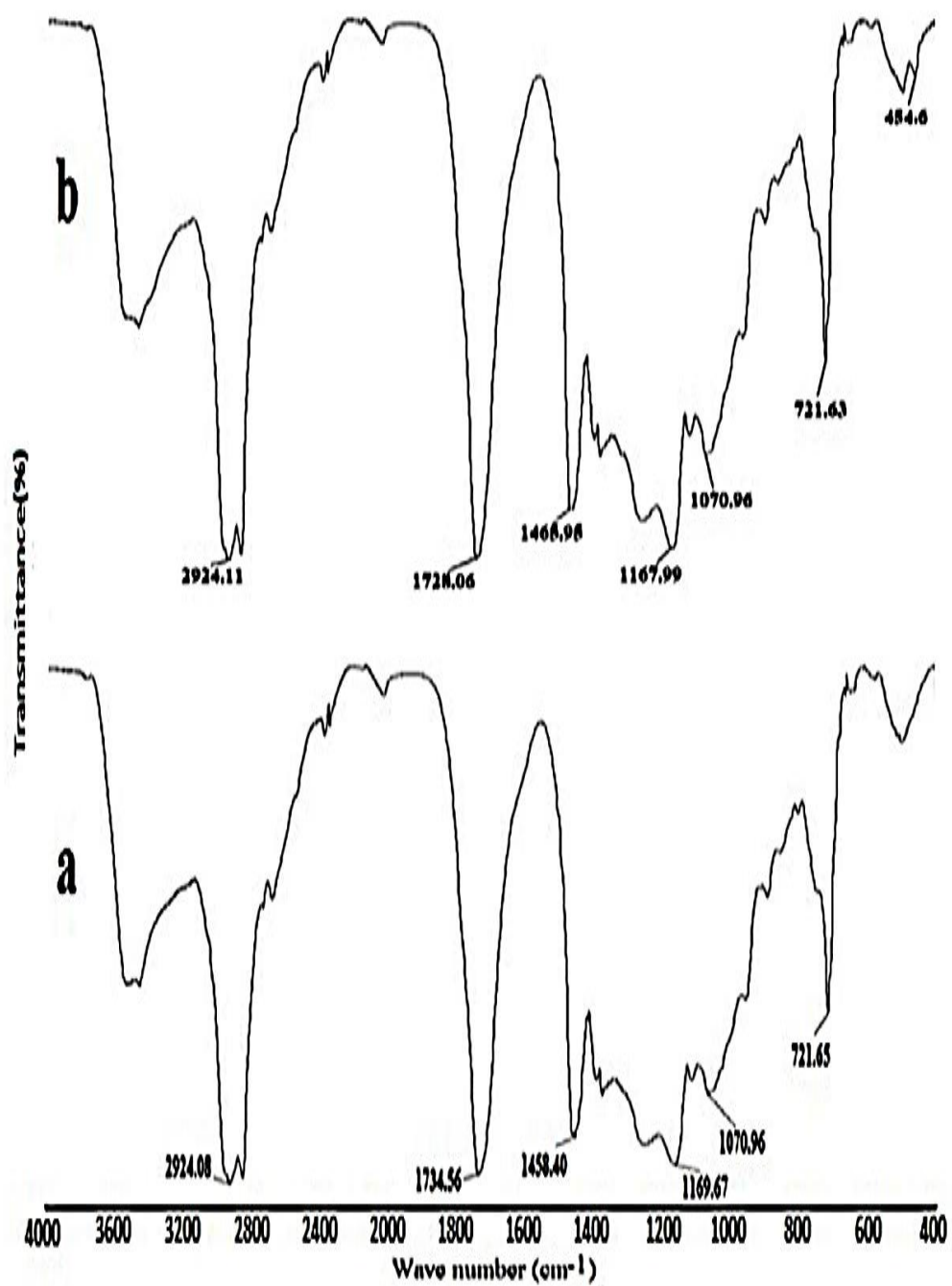


Figure 1.5.1: FT-IR spectra of (a) polymer (A) and (b) polymer/ZnO nano composite (Z-3)

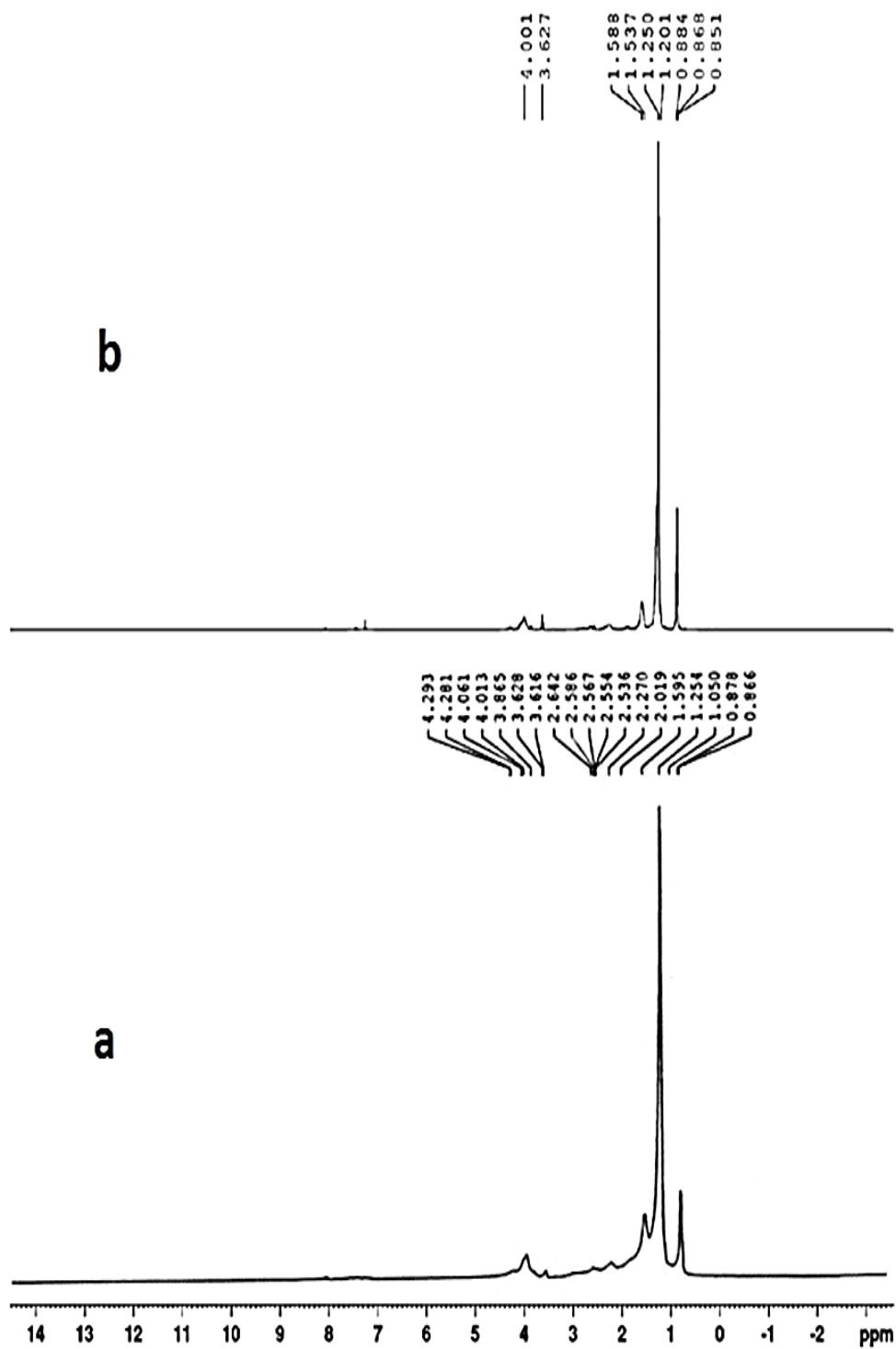
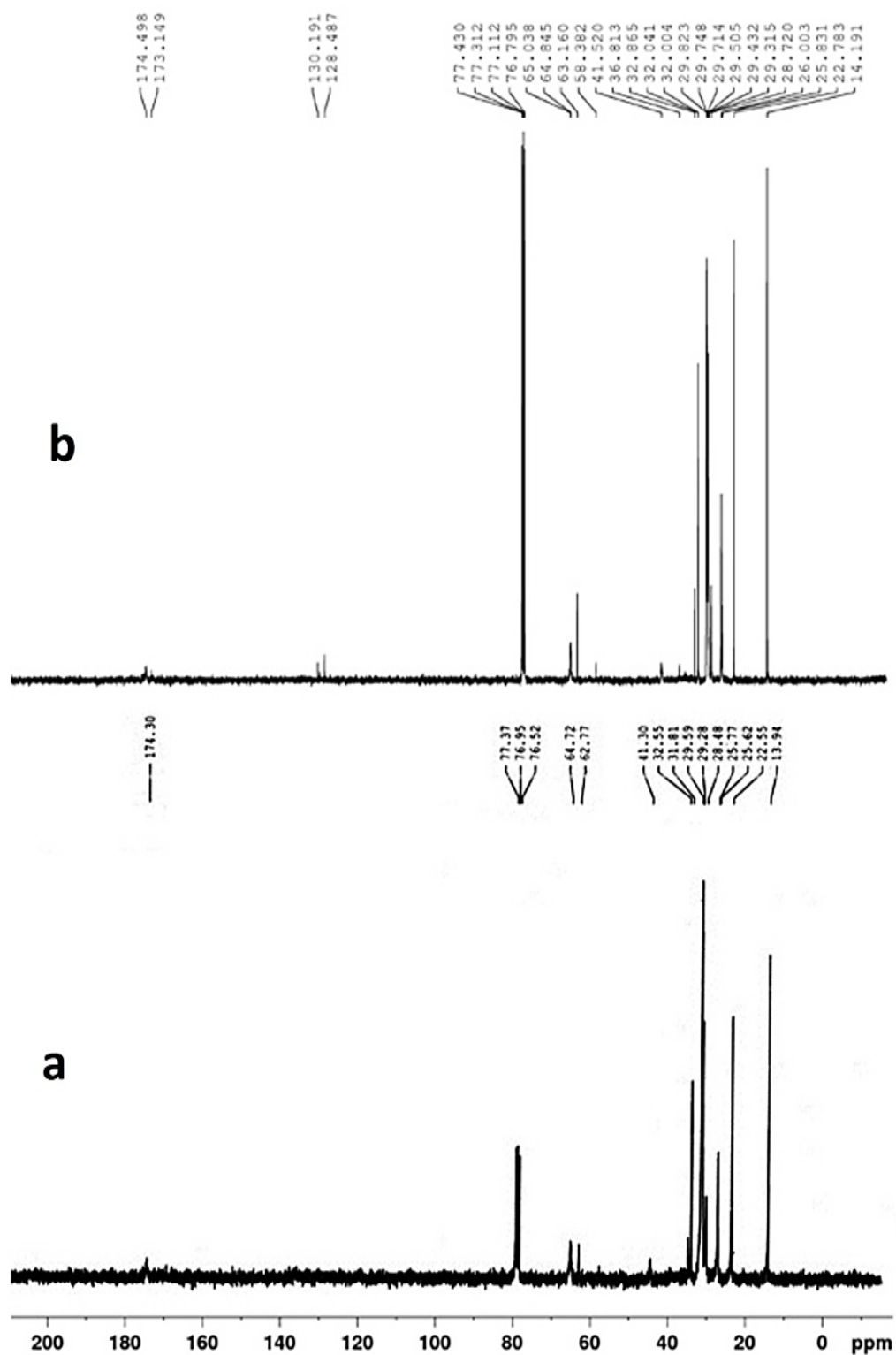


Figure 1.5.2:  $^1\text{H}$  NMR spectra of polymer (A) and the PNC (Z-3)



**Figure 1.5.3:**  $^{13}\text{C}$  NMR spectra of polymer (A) and the composite (Z-3)

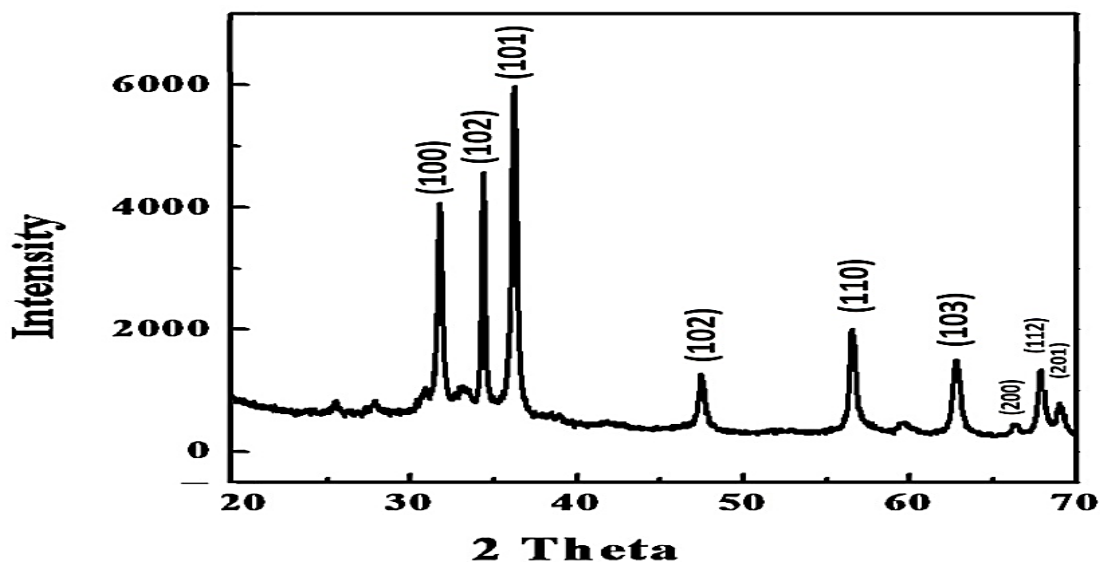


Figure 1.5.4 XRD spectra of prepared ZnO nanoparticles

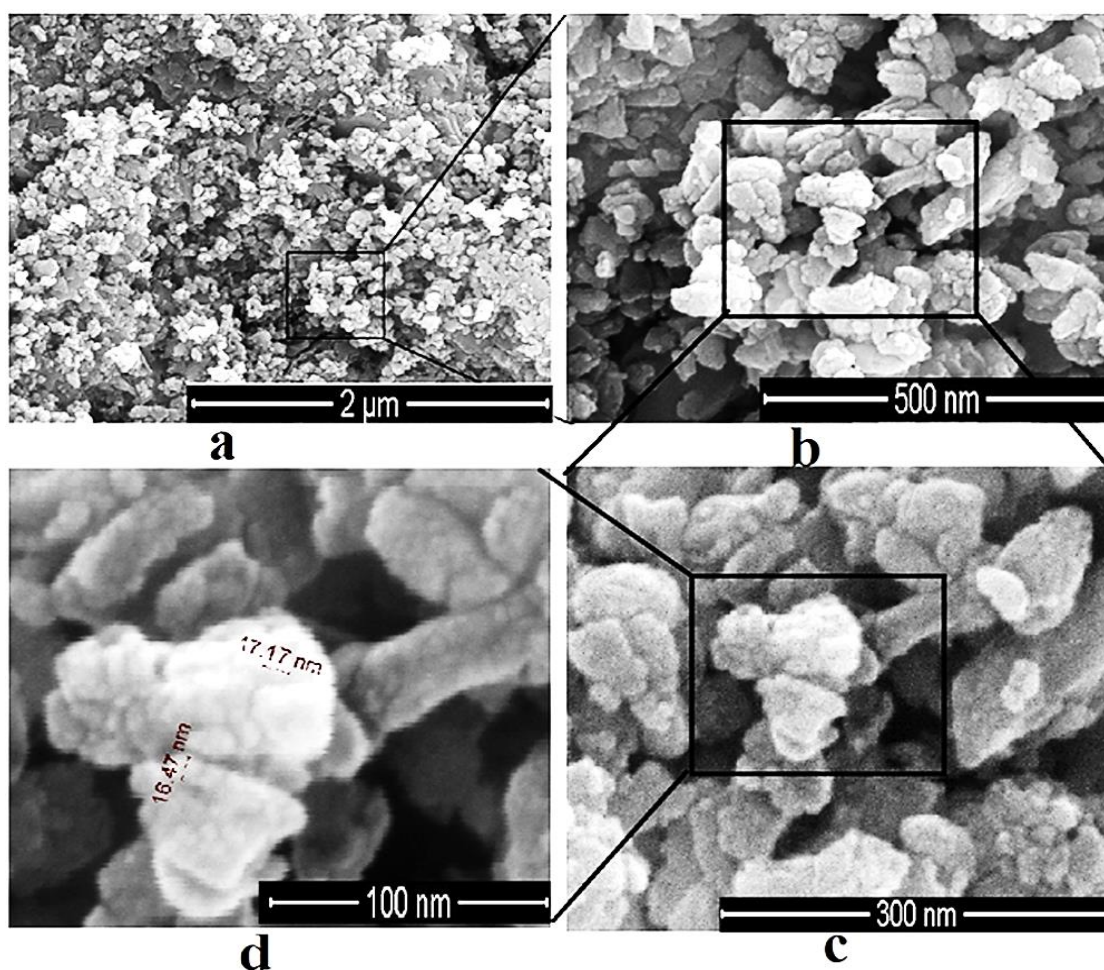


Figure 1.5.5: SEM images (a, b, c and d) of prepared ZnO nanoparticle at different magnifications

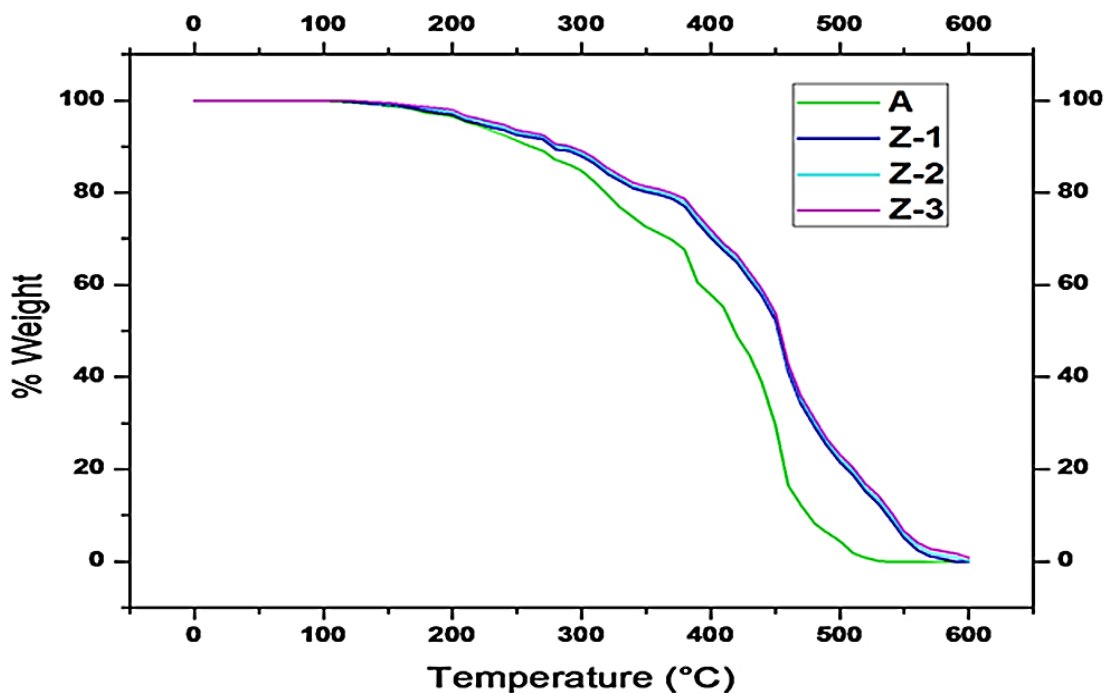


Figure 1.5.6: TGA data of polymer (A) and polymer/ZnO nanocomposite (Z-1, Z-2 and Z-3)

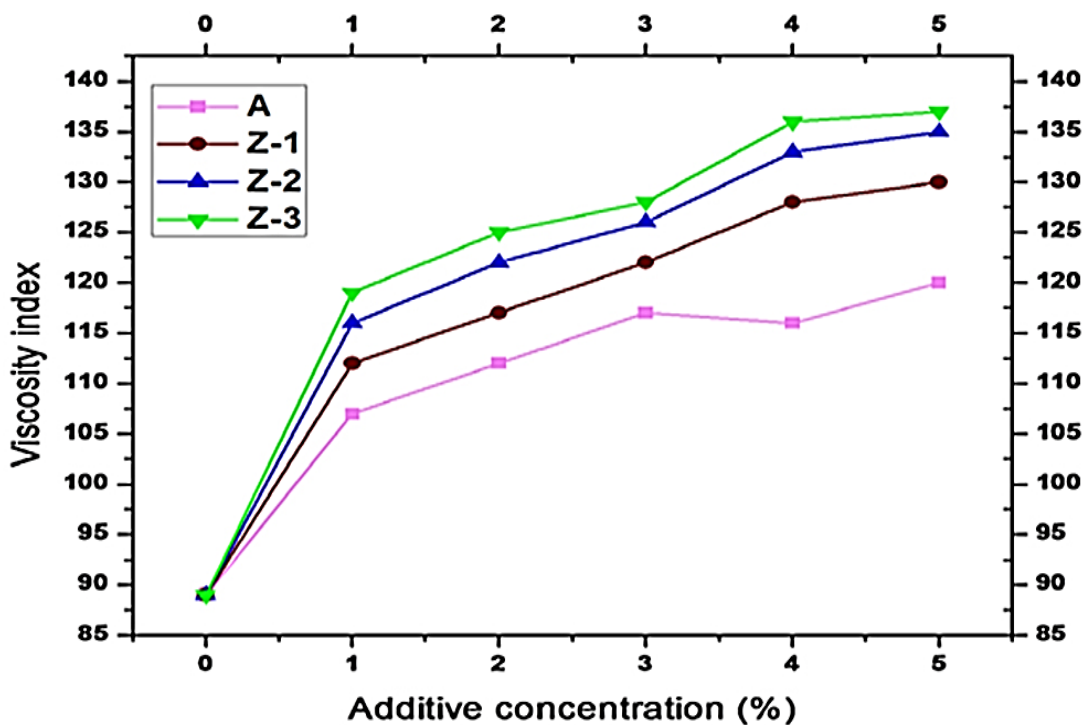


Figure 1.5.7: Plot of viscosity index of the lube oil blended with additives at different concentration levels

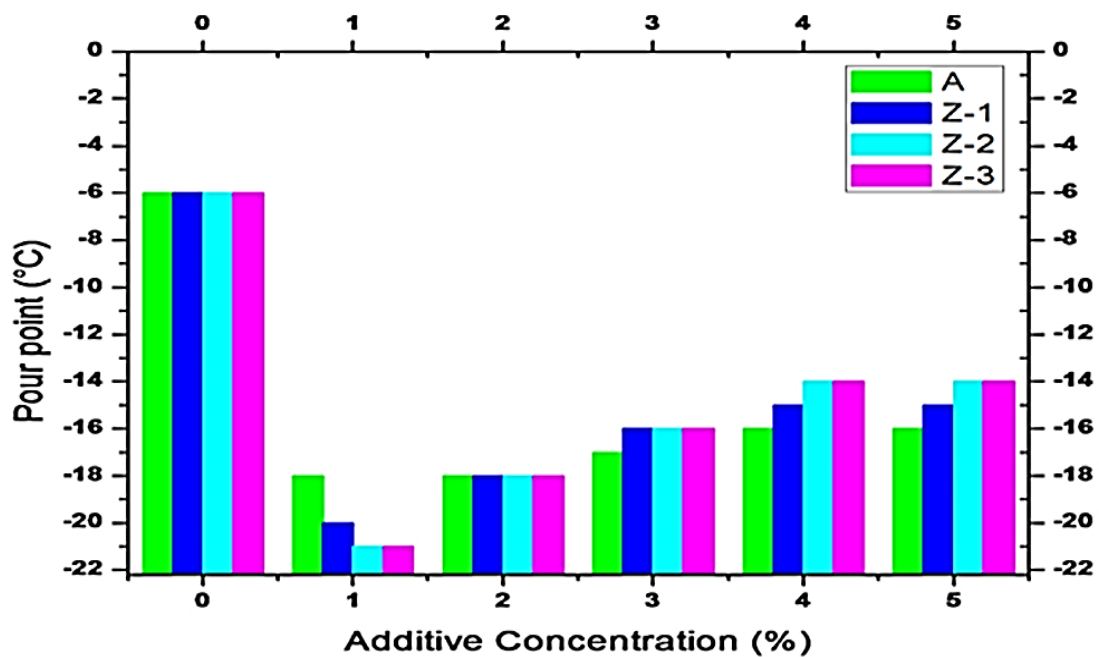


Figure 1.5.8: Plot of pour point of the lube oil blended with additives at different concentration

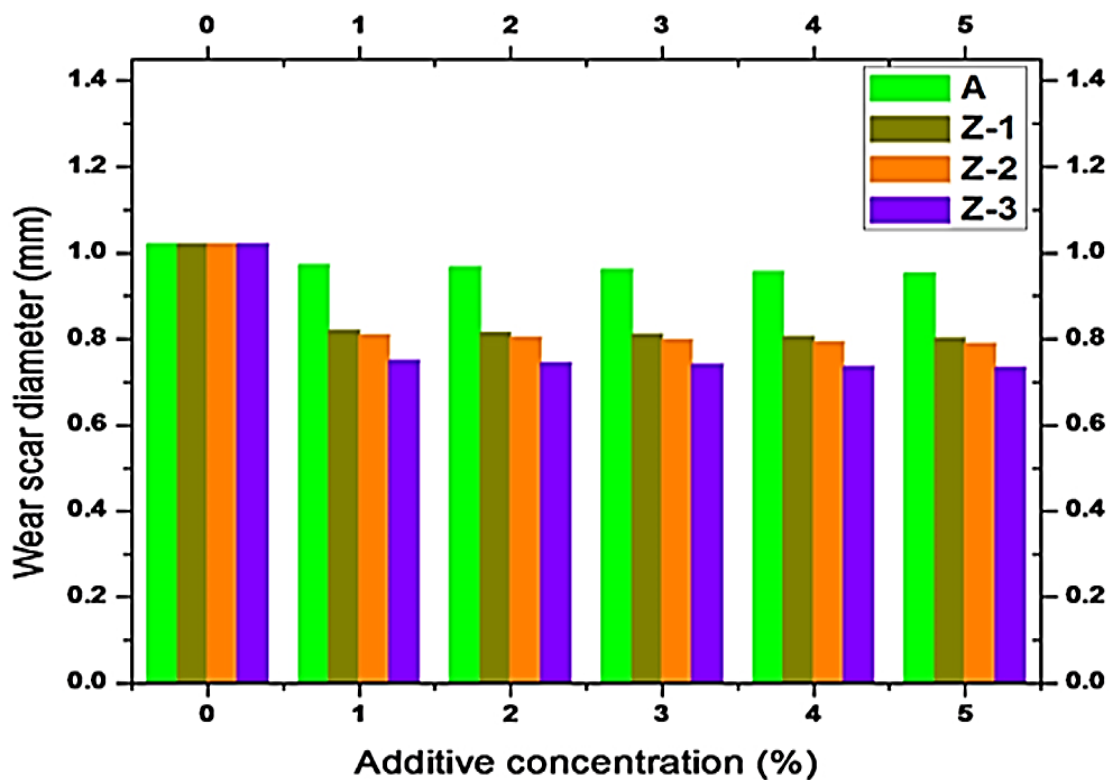


Figure 1.5.9: Wear scar diamete